

Fabrication and Characterization of Bimetallic Modified Biochar

Zhigen Li* Junjie Dai

School of Life and Environmental Sciences, Shaoxing University, Shaoxing, 312000, China

Abstract. This study presents the fabrication and characterization of Fe-Mn bimetallic oxide-modified corn stalk biochar (FM@BC) for the removal of Cd(II) from aqueous solutions. The biochar was synthesized via oxygen-limited pyrolysis at 600°C, followed by chemical impregnation with iron and manganese salts. SEM-EDS analysis confirmed successful modification, revealing corroded surfaces with aggregated particles and altered pore structures compared to pristine biochar. Adsorption experiments demonstrated that Cd²⁺ uptake increased progressively over time, reaching a maximum capacity of 112.5 mg/g. Kinetic modeling indicated that the pseudo-second-order model provided the best fit ($R^2 > 0.99$), suggesting chemisorption as the dominant mechanism. Isotherm studies showed that the Langmuir model fitted the data better than the Freundlich model ($R^2 = 0.984$), indicating monolayer adsorption on homogeneous surfaces. Speciation analysis revealed that free Cd²⁺ ions predominated at pH < 8, while Cd(OH)₂ precipitation occurred at pH > 8. The bimetallic modification effectively enhanced Cd(II) removal efficiency by overcoming the limitations of unmodified biochar. This cost-effective and environmentally sustainable approach utilizing agricultural waste biomass demonstrates significant potential for remediating Cd-contaminated water and soil, contributing to sustainable environmental management practices.

1 Introduction

Soil is an essential natural component of terrestrial ecosystems and serves as the foundation for sustainable agricultural development. However, soil heavy metal pollution has become a global issue. According to preliminary statistics from scholars, the total amount of cadmium (Cd) emitted into the environment globally over the past few decades has reached 2.2×10^4 tons. Research by Khan et al. indicates that the average Cd content in French soils is $16.7 \text{ mg} \cdot \text{kg}^{-1}$, while in Belgian soils it is $7.61 \text{ mg} \cdot \text{kg}^{-1}$, and in Chinese soils, it is $7.43 \text{ mg} \cdot \text{kg}^{-1}$ [1]. In Japan, there are numerous cases of heavy metal pollution from old mines and smelters, and heavy metal contamination in agricultural soils has become a serious social issue[2].

Biochar is a porous carbon-rich material formed through the anaerobic pyrolysis of biomass. Based on its high efficiency, moderate cost, and wide applicability, adsorption technology has become one of the important methods for treating heavy metal-contaminated soils[3]. Furthermore, the application of biochar increased the total nitrogen, organic matter, and available potassium content in the soil, highlighting the significant role of biochar in enhancing soil fertility and improving the ecological environment. Unmodified pristine biochar exhibits limited remediation efficacy for Cd contamination, particularly due to the constraints of surface negative charges. Therefore, enhancing biochar's Cd remediation performance requires modification. Metal loading-including zero-valent iron, FeSO₄, KMnO₄, FeCl₃, and

goethite-is a common approach[4]. Feng et al. found that biochar modified with FeSO₄ showed increased iron and sulfur content, as well as a higher specific surface area. The removal rates of multi heavy metals using biochar modified with FeCl₃ improved obviously. Luo et al. modified biochar with TiO₂ to simultaneously remove Cd(II) and As(V) from water, achieving maximum adsorption capacities of 72.62 mg/g and 118.06 mg/g, which were three times higher than those of unmodified biochar[5].

Several studies have investigated the adsorption of wastewater by modified biochar. Lou et al. synthesized magnetic rice husk biochar through high-temperature carbonization, hydrofluoric acid desilication, zinc chloride activation, and in-situ chemical co-precipitation with Fe³⁺ and Fe²⁺[6]. Although this adsorbent exhibited excellent adsorption capacity for tetracycline, issues associated with its production and application still require attention and resolution. To address these challenges, researchers may explore more environmentally friendly and economically viable modification methods, seek alternative and less toxic modifying reagents, or optimize the process to reduce reagent consumption and waste generation[7]. Li prepared renewable biochar from rice husk via hydrothermal treatment and KMnO₄ activation, which effectively removed dyes from wastewater. Herrera et al. found that pyrolyzed rice husk achieved removal efficiencies exceeding 95% for both azithromycin and erythromycin. Based on current research, rice husk biochar demonstrates promising efficacy for the removal

* Corresponding author: zhigen.li@usx.edu.cn

of high-molecular-weight contaminants from water sources, warranting further investigation[8].

2 Materials and Methods

2.1 Biochar Preparation

The biochar was prepared as the method stated below: Corn stalks were rinsed with deionized water, air-dried for 7 days, and then crushed to 1-2 mm to obtain crushed corn stalks. The crushed corn stalks were placed in a muffle furnace and pyrolyzed at 600°C under a nitrogen (N₂) atmosphere. Ten grams of biochar were added to 200 mL of a mixed solution containing Fe(NO₃)₃·9H₂O and KMnO₄. The surface morphology and elemental distribution of biochar and modified biochar were characterized using scanning electron microscopy coupled with energy-dispersive X-ray spectroscopy (SEM-EDS) (SU8020, Hitachi, Japan). The elemental composition (C, H, N, S, O) of the adsorbent samples was determined using an elemental analyzer (Elementar VARIO EL cube, Germany).

2.2 Effect of Contact Time on Cd²⁺ Adsorption and Adsorption Kinetics Studies

Biochar Adsorption Experiment: 50 mg of biochar adsorbent was added to 30 mL of Cd stock solution with an initial concentration of 80 mg/L. The mixture was stirred/oscillated for a specified duration to ensure adequate contact between biochar and cadmium ions. The solution pH was adjusted to 6.0 using 0.01–1.0 M HCl or NaOH. The reaction mixture was then placed in a temperature-controlled shaking incubator at 25 °C, and the reaction was allowed to proceed continuously after adsorbent addition. Samples were collected at predetermined time intervals of 5, 10, 15, 20, 40, 50, 90, 120, 240, 300, 360, 420, and 480 min. At each time point, 5 mL aliquots were drawn in triplicate (total 15 mL) using a syringe and filtered through 0.22 μm syringe filters to remove any solid particles or impurities. The filtered solutions were transferred to centrifuge tubes for subsequent concentration determination. In practical applications, the most appropriate kinetic model should be selected based on specific experimental conditions, whether it is the pseudo-first-order or pseudo-second-order kinetic equation:

The pseudo-first-order kinetic equation is expressed as follows:

$$\ln(q_e - q_t) = \ln q_e - k_1 t$$

The pseudo-second-order kinetic equation is expressed as follows:

$$\frac{t}{q_t} = \frac{1}{k_2 q_e^2} + \frac{t}{q_e}$$

Where: *t* represents the adsorption time (min); *k₁* is the rate constant of the pseudo-first-order kinetic equation (min⁻¹); *q_e* is the equilibrium adsorption capacity of the adsorbent (mg·g⁻¹); *q_t* is the adsorption capacity of the adsorbent at time *t* (mg·g⁻¹); and *k₂* is the rate constant of the pseudo-second-order kinetic equation (g·mg⁻¹·min⁻¹).

2.3 Effect of Initial Concentration on Cd²⁺ Adsorption and Adsorption Isotherm Thermodynamics Studies

Solution preparation: the Cd stock solution was diluted to the desired concentrations (ranging from 20 to 120 mg/L at 20 mg/L intervals, yielding six concentration levels). For each concentration, 30 mL of solution was prepared and mixed with 50 mg of adsorbent material. The pH was adjusted to 6.0, and the mixtures were shaken at a constant temperature of 25 °C for 6 h. Subsequently, 10 mL of each solution was extracted using a 5 mL disposable needle-free syringe, filtered through a 0.22 μm aqueous-phase filter, and transferred into 15 mL centrifuge tubes for subsequent analysis.

The Langmuir model equation is expressed as follows:

$$\frac{1}{q_e} = \frac{1}{q_{max}} + \frac{1}{q_{max} K_L C_e}$$

The Freundlich model equation is expressed as follows:

$$\ln q_e = \ln k_F + \frac{1}{n} \ln C_e$$

Where: *q_e* represents the equilibrium adsorption capacity (mg·g⁻¹); *q_{max}* represents the maximum adsorption capacity (mg·g⁻¹); *C_e* represents the equilibrium concentration of metal ions in solution (mg·L⁻¹); *b* represents the Langmuir constant related to adsorption energy (L·mg⁻¹); and *K_F* and *n* are Freundlich constants related to adsorption capacity and adsorption intensity, respectively (with *K_F* in mg·g⁻¹ and *n* dimensionless).

3 Results and Discussion

Unmodified pristine biochar exhibits limited remediation efficacy for Cd contamination, particularly due to the constraints of surface negative charges. Therefore, enhancing biochar's Cd remediation performance requires modification. Metal loading-including zero-valent iron, FeSO₄, KMnO₄, FeCl₃, and goethite-is a common approach. Feng et al. found that biochar modified with FeSO₄ showed increased iron and sulfur content, as well as a higher specific surface area. The removal rates of multi heavy metals using biochar modified with FeCl₃ improved obviously[9].

The surface morphology features and elemental composition of BC and FMBC are shown in Fig.1. From the SEM images, the biochar derived from corn stalks exhibits a clear long-fiber structure on its surface, with a smooth surface and uniform pore structure, which is consistent with previous reports. The biochar is mainly composed of C, O, Mg, Si. However, after Fe-Mn impregnation-modification, the surface of the biochar becomes corroded and its pore structure is disrupted, with a large number of agglomerated particles distributed on the surface.

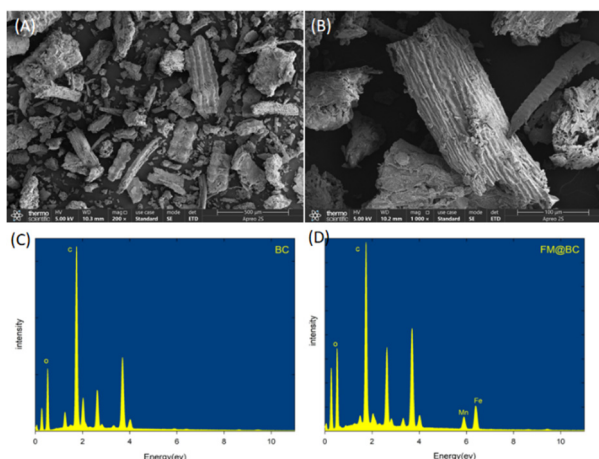


Fig.1 SEM detection results of original and modified rice straw biochar. Image of Fe/Mn bimetallic oxide modified biochar (A); original biochar (B); EDS of BC (C), FM@BC (D).

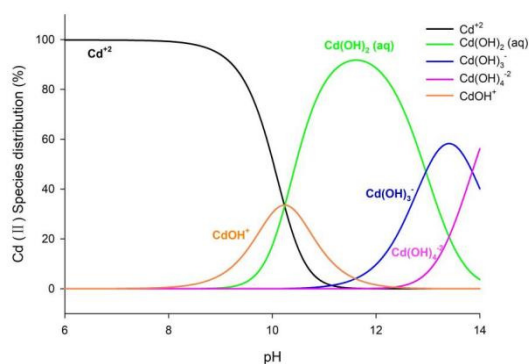


Fig.2: The Cd(II) speciation in different pH of the aqueous solution using Visual MINTEQ.

This image presents the pH-dependent speciation distribution of Cd(II) species in aqueous solution, generated using Visual MINTEQ software. When acidic to neutral pH (pH 6-9), Cd^{2+} dominates completely, accounting for nearly 100% of total Cd species. This indicates that under acidic and neutral conditions, Cd remains predominantly in its dissolved ionic form. As pH increases to 9-11, Cd^{2+} concentration decreases sharply. Concurrently, CdOH^+ (orange curve) emerges as a transient species, peaking around pH 10 at approximately 33% distribution. Simultaneously, Cd(OH)_2 (aq) (green curve) begins to form and increases rapidly. Cd(OH)_2 (aq) becomes the predominant species, reaching its maximum distribution of approximately 90% around pH 11.5. This represents the optimal pH range for cadmium hydroxide formation in aqueous solution.

The diagram demonstrates that for effective Cd^{2+} adsorption onto biochar materials, maintaining pH below 8 is crucial to ensure cadmium exists primarily as free Cd^{2+} ions. At $\text{pH} > 8$, various hydroxide species and precipitation become significant, which would complicate the adsorption mechanism interpretation. This validates the experimental design choice of pH 6.0 in your biochar adsorption experiments, where Cd^{2+} exists predominantly as free ions, enabling clear assessment of the adsorption process without interference from precipitation phenomena. The distribution diagram of Cd(II) shows that,

when $\text{pH} < 8$, Cd in solution predominantly exists as Cd^{2+} , whereas at $\text{pH} > 8$, most Cd^{2+} is precipitated, with Cd(OH)_2 being the primary species present (Fig.2).

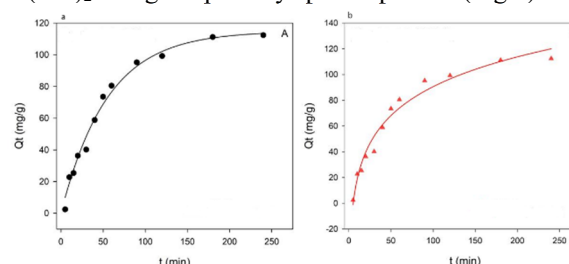


Fig.3: Quasi-first-order dynamics (a) and quasi-second-order dynamics model (b).

The adsorption kinetic experimental results show that the adsorption capacity of Cd^{2+} increased gradually over time, with the modified material exhibiting a relatively fast adsorption rate. The adsorption capacity of Cd^{2+} rose rapidly during the initial stage, subsequently decelerated, and eventually reached saturation, with a maximum adsorption capacity of 112.5 mg/g (Fig.3). Fitting analysis revealed that the pseudo-second-order kinetic model provided a better fit, indicating that the adsorption of Cd^{2+} by the modified material conformed more closely to the pseudo-second-order kinetic model. This suggests that chemisorption played a dominant role in the adsorption process, which is associated with the interaction between the adsorbent and adsorbate. The adsorption characteristics of biochar for Cd^{2+} and their influencing factors are complex and diverse, encompassing Cd^{2+} concentration, the physicochemical properties of biochar, and other environmental factors. These elements collectively determine the activity of adsorption sites on the biochar surface and the ultimate attainment of equilibrium[10].

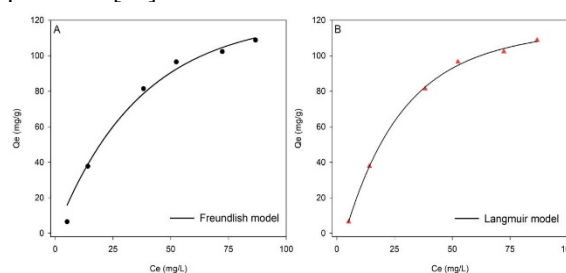


Fig.4: Freundlich Model Fitting (a), Langmuir Model Fitting (b).

The Langmuir and Freundlich models are two important isothermal adsorption models in adsorption science. The Langmuir model is applicable to monolayer physical adsorption under ideal conditions, whereas the Freundlich model is more suitable for describing multilayer chemical adsorption that may occur under practical conditions (Fig.4). Although these two models can be used interchangeably in certain cases, their fundamental assumptions and applicable scopes differ significantly.

As shown in the figure above (Fig.4), the adsorption process of Cd^{2+} by biochar proceeded from rapid to slow, which was primarily attributed to the pore structure of the

biochar surface and the variation in concentration gradient, with the solute serving as the main driving force. During the initial stage of adsorption, the adsorption rate was extremely rapid due to the abundance of available adsorption sites on the biochar surface and the high concentration gradient between the solution and the biochar surface, resulting in a steep kinetic curve. However, as time progressed, these adsorption sites were gradually occupied and the concentration gradient diminished, leading to a decreased adsorption rate and a flattening of the kinetic curve, thereby entering the slow adsorption stage. This phenomenon may be associated with the presence of adsorption sites with varying energy levels on the biochar surface. These findings indicate that rapid adsorption is of significant importance for enhancing the adsorption efficiency of biochar and removing cadmium ions from water.

To investigate the adsorption of Cd^{2+} from aqueous solution by modified rice husk biochar, the two aforementioned models were employed to analyze the experimental results. The horizontal axis represents the equilibrium concentration, and the vertical axis represents the equilibrium adsorption capacity, with both models fitted to the data. Calculations revealed that the Langmuir model exhibited a higher R^2 value (0.984). It can be observed that the Langmuir isothermal adsorption model provided a superior fit compared to the Freundlich isothermal adsorption model, indicating that the Langmuir model is more appropriate for describing the adsorption process of Cd^{2+} from aqueous solution by modified rice husk biochar. The Langmuir model assumes a homogeneous monolayer of adsorbed molecules on the adsorbent surface; if experimental data demonstrate a uniform adsorbent surface, minimal variation in adsorption heat, low surface coverage, and moderate pressure, fitting with the Langmuir isothermal adsorption model may yield greater accuracy, with no interaction between adsorbed molecules. Therefore, the adsorption of Cd^{2+} from aqueous solution onto modified rice husk biochar was primarily dominated by monolayer adsorption. Further analysis of the Langmuir model fitting parameters revealed that the theoretical maximum adsorption capacity approached or even slightly exceeded those of common activated carbon and attapulgite, demonstrating that this modified rice straw biochar exhibited exceptional adsorption performance for Cd^{2+} in aqueous solution[11].

4 Conclusion

This study successfully prepared Fe-Mn bimetallic oxide-modified corn stalk biochar (FM@BC) through oxygen-limited pyrolysis at 600°C followed by chemical impregnation with iron and manganese salts. The SEM-EDS characterization confirmed successful modification, revealing corroded surfaces with aggregated particles and altered pore structures compared to pristine biochar. The pH-dependent speciation analysis demonstrated that Cd(II) predominantly exists as free Cd^{2+} ions at pH below 8, while precipitation as $\text{Cd}(\text{OH})_2$ occurs under alkaline conditions above pH 8, which is crucial for understanding

adsorption mechanisms. The bimetallic modification strategy effectively addresses the limitations of unmodified biochar, particularly its constrained surface negative charges, thereby significantly enhancing Cd(II) removal efficiency from aqueous solutions. This approach offers multiple advantages including utilization of agricultural waste biomass, cost-effectiveness, and environmental sustainability. The FM@BC material demonstrates considerable potential for practical applications in remediating Cd-contaminated soils and wastewater, contributing to sustainable agricultural development and ecosystem protection. Future research should focus on optimizing modification parameters, evaluating long-term stability, and assessing field-scale remediation performance to facilitate industrial application of this promising adsorbent material.

Acknowledgement

Funding This research was supported by Zhejiang Province Shaoxing Basic Public Welfare project under Grant No.2023A12002 and Zhejiang Provincial Department of Education research project No.Y202454793.

Contribution: Zhigen Li: Conceptualization, Formal analysis, Investigation, Writing an original draft. Junjie Dai: Data curation, Methodology.

References

1. Regmi P, Garcia Moscoso J L, Kumar S, et al. *Journal of Environmental Management*, 2012, 109:61-69.
2. Zhou Q W, Liao B H, Lin L N, et al. *Science of the Total Environment*, 2018,615:115-122.
3. Zhang X, Lyu L, Qin Y Z, et al. *Bioresource Technology*, 2018,256:1-10.
4. Yin G C, Song X W, Tao L, et al. *Chemical Engineering Journal*, 2020,389:124465.
5. Wang M C, Sheng G D, Qiu Y P. *International Journal of Environmental Science and Technology*, 2015,12(5):1719-1726.
6. Yang F, Zhang S S, Sun Y Q, et al. *Bioresource Technology*, 2018,265:490-497.
7. Higashikawa, Fábio Satoshi, Conz R F , Colzato M , et al. *Journal of Cleaner Production*, 2016, 137:965-972.
8. Ngah W S W , Hanafiah Makm. *Bioresource Technology*, 2008, 99(10):3935-3948.
9. Pan J , Jiang J , Xu R . *Journal of Environmental Sciences*, 2013, 25(10):1957-1965.
10. Xu X , Cao X , Zhao L. *Chemosphere*, 2013, 92(8):955-961.
11. Lou K , Rajapaksha A U , Ok Y S , et al. *Chemical Speciation & Bioavailability*, 2016, 28(1-4):42-50.